Opportunities for 3D printed millifluidic platforms incorporating on-line sample handling and separation

David J. Cocovi-Solberg*[a], Paul J. Worsfold*[b], and Manuel Miró*[a]

[a] FI-TRACE Group, Department of Chemistry, University of the Balearic Islands, Carretera de Valldemossa km 7.5, E-07122 Palma de Mallorca, Illes Balears, Spain.

[b] Biogeochemistry Research Centre, SoGEES, Plymouth University, Plymouth PL48AA, Devon, UK.

* Corresponding authors.
E-mail: david.cocovi@uib.es; dj.cocovi.solberg@gmail.com (D.J. Cocovi-Solberg)
E-mail: p.worsfold@plymouth.ac.uk (P.J. Worsfold)
E-mail: manuel.miro@uib.es (M. Miró)

Abstract

3D printing is an emerging enabling technology that can facilitate the production of complex 3D structures in analytical chemistry, including the millifluidic, e.g. flow injection (FI), and microfluidic arenas. In this review, the potential of 3D printing for the fabrication of cost-effective millifluidic platforms incorporating on-line sample handling and separation is critically appraised against traditional configurations or manufacturing processes. Applications resorting to structures achievable with 3D printing, in some instances exploiting the surface chemistry of the printable material, are grouped under: (i) fluidic drivers, mixers and reactors; (ii) membrane separation, (iii) sorbent extraction/concentration, (iv) chromatographic and electrophoretic separation, and (v) sensing and detector housings. Summary tables are also presented for reported applications of on-line sample handling and separation in environmental and biochemical analysis.

List of abbreviations

2D	2-dimensional
3D	3-dimensional
ABS	Acrylonitrile-butadiene-styrene
CAD	Computer assisted design
CAM	Computer assisted modelling
DLP	Digital light processing
FDM	Fused deposition modelling
FI	Flow injection
ICP-MS	Inductively coupled plasma-mass spectrometry
i.d.	Internal diameter
MIP	Molecularly imprinted polymer
NP	Nanoparticle
PCL	poly-ε-caprolactone
PDMS	Polydimethylsiloxane
PIP	Photopolymer inkjet printing
PLA	Polylactic acid
PVA	Polyvinyl alcohol
SLA	Laser-based stereolithography
SLM/S	Selective laser melting/sintering
SPE	Solid phase extraction

1. Introduction

Three-dimensional (3D) printing is an emerging and enabling technology in analytical science used for the fabrication of three dimensional analytical devices and platforms based on additive manufacturing [1-7], that is, the material is being added, rather than subtracted, to create custom devices. The main advantages of 3D printing are the capability of fabricating components and integrated platforms that cannot easily be manufactured by conventional means [e.g. 8, 9, 10], e.g. by traditional milling, and the fact that the object is printed in a single step, usually with no need for postprinting chemical treatment. Further benefits that foster the implementation of 3D printing in the analytical science domain are (i) rapid prototyping, (ii) low start up and running costs and (iii) advances in CAD/CAM software that allow a very intuitive operation, i.e. analytical scientists can produce bespoke platforms and integrated devices for a range of analytical applications [4]. These include microfluidic (lab-on-a-chip) devices [2], which typically contain <500 μm i.d. channels, as well as millifluidic (>1 mm) and sub-millifluidic (0.5 – 1 mm) devices, such as flow injection (FI) platforms [8, 11-14]. In fact, milled fluidic structures can only be fabricated using several steps that require technical intervention and/or expensive 5-axis mills, and intricate structures cannot be designed without gluing or fastening together individual components. 3D printing also offers the possibility of fabrication of low-performance devices for educational purposes in undergraduate analytical chemistry courses, as exemplified by the fabrication of a filter fluorimeter [15].

Detailed descriptions of the technological approaches to 3D printing and critical comparisons of performance for milli/microfluidic platforms are provided in several reviews [e.g. 2, 3, 4, 7, 16-19]. In addition, several articles describe practical aspects and innovative approaches for fabrication [e.g. 5, 16, 20-25]. As a résumé of those review papers, fused deposition modelling (FDM), based on the extrusion of heated thermoplastic filaments, features the widest choice of printable materials, with polylactic acid (PLA) and acrylonitrile-butadiene-styrene (ABS) being the most widely used [26]. FDM is also characterized by relatively low start-up and running costs with multi-material printing capability, but at the expense of slow build workflows. Post-processing is required to make devices air-tight by e.g. high-temperature treatment or soaking in acetone [27], but this may compromise fluidic features such as channel cross-sectional area and wall thickness. Stereolithography encompasses laser-based stereolithography (SLA), based on layer-by-layer photopolymerization of a (normally) proprietary epoxy acrylate-based resin by a scanning laser, and digital light processing (DLP), in which the UV source passes across a digital mask. DLP and SLA are characterized by slightly higher printer and running costs compared with FDM but render smoother surfaces (excellent for laminar flow features), fast post-processing and transparent prints. The performance characteristics of FDM, DLP, SLA and also inkjet printing have been critically compared by Macdonald *et al.* in terms of size, accuracy, suitability for mass manufacturing and surface smoothness [28]: DLP has good resolution for open channels because the light modulation is performed with a steady projector, rather than movable galvanometers, but has limited build space, and hence throughput, making it most suitable for single-device prototyping or small batch production. Photopolymer inkjet printing (PIP, often referred to as PolyJet (Stratasys®) or MultiJet (3D Systems®)), using photo-curable liquid resins, is appropriate for multi-material printing and for the fabrication of micro- and sub-millifluidic devices. PIP can fabricate the smallest closed channels (≥ 205 ± 13 μm, unless custom-built printers with their own light sources

and specifically-designed and optimized resin formulations are used [29]), with a high throughput (≤ 33 fluidic platforms per hour [28]), but at the expense of elevated start-up costs and lengthy post-processing procedures to remove the support material, which may be troublesome for narrow bore or spiral-shaped channels. Another approach to 3D printing is selective laser melting or sintering (SLM/S) based on melting of deposited metal powder or sintering of deposited metal/polymer powder to create metal-based fluidic components, such as holders for chromatographic separation [9].

Traditional machining can use virtually any material, but the range of 3D printing materials is still very limited, which is the main constraint for this technique to offer wide opportunities for mass applicability of printed structures. As detailed above, PLA, ABS and acrylate-based polymers are the most common materials but their limited chemical compatibility with organic solvents restricts the application of the prints for non-aqueous (bio)chemical assays. In general, polymeric materials are not fully compatible with halogenated or low-molecular weight polar solvents for prolonged exposition times (e.g., acetonitrile, acetone). Those caveats could be addressed using non-polymeric/metal printable materials [9, 30] or by protection of the inner surfaces with printed-in coatings that concomitantly can serve as chemical reagents [6, 10]. In fact, most of the treatments reported in the literature aim at tuning the surface chemistry of the prints (e.g., by covalent binding of reactive moieties [31, 32], see also below), to endow entirely new properties for chemical reactors.

The main fluidic parameters to explore in 3D prints include minimum channel cross-section, post-processing requirements, transparency, durability, channel porosity, surface roughness and chemical compatibility with samples and reagents. Biocompatibility of materials is sometimes addressed [33], but in the analytical chemistry domain it is almost meaningless, since the term resorts to the ability of living tissues to tolerate or grow onto materials, and biological samples are in contact with the printed material of fluidic structures for a short time. The cost of the substrate and power consumption, build speed and throughput of production are only relevant for scale-up fabrication.

While previous reviews have focused on the fabrication of 3D printed devices intended for proof-of-concept fluidic applications, this review focuses on the strategies used to incorporate sample handling and separation in 3D printed milli/mesofluidic platforms. A particularly attractive feature of 3D printing for analytical chemists and practitioners working with millifluidic devices, such as FI and variants thereof, is the ability to design and rapidly fabricate unique bespoke components including fluidic drivers and reactors for on-line automatic sample handling and separation prior to detection, as discussed below. A conceptual FI manifold showing examples of 3D printed devices for on-line membrane separation, sorbent extraction/concentration and chromatographic/electrophoretic separation is shown in Fig. 1.

2. Fluidic drivers, mixers and reactors

The 3D printing of a variety of individual microfluidic and millifluidic actuators, flow components and interfaces has been reported in the literature, including (manually

operated) torque-actuated pumps and valves [34], load/inject valves [35], diaphragm valves [36-38], pumps based on serially operated diaphragms [36, 39], knotted/serpentine reactors [40], reactionware devices for organic synthesis under flow-chemistry conditions [6, 41, 42] and even modular distillation columns [10]. Two examples of 3D printed reactors with meandering stream channel patterns and a 3D printed lab-on-valve stator are illustrated in Fig. 2. On-line mixing of sample with reagent(s) and sample dilution are two of the most basic features of milli/microfluidic systems and components to carry out these key operations can be 3D printed. For example, fully automated, one-step DLP printing of complex device designs at a speed of 20 mm h^{-1} in height were achieved for sizes up to 43 mm × 27 mm × 180 mm (x × y × z) [22]. The x, y and z resolutions were ≈50 µm and the smallest enclosed channel dimensions were 250 x 250 µm. Mixing and gradient formation components were incorporated into a 3D printed microfluidic device for the spectrophotometric determination of nitrate in tap water using the Griess chemistry. Flow was driven by syringe pumps for this application and multiple depth detection cells were used to extend the linear range [22].

With respect to diverting valves and liquid drivers, valves with moving parts and membrane-based (20 µm thickness) diaphragm pumps have been 3D printed with acrylic based formulations using DLP and combined to provide mixers and multiplexers in fluidic structures [36]. For example, a 3-to-2 multiplexer was used to pump aqueous solutions (at 40 µL min^{-1}) from any three inputs to any two outputs via a displacement chamber. Build layer thickness was 10 µm and the microfluidic channel cross section was 150 µm high and 162 µm wide [36]. SLA has also been used with a proprietary ABS-like resin to 3D print fluidic valves and pumps in optically-clear polymer, which were integrated within low cost microfluidic devices for biomedical applications [39]. To operate the valves, pressurised air (1 - 6 psi) was used to deflect a membrane (1 cm diameter) which opened and closed a circular cross-section microfluidic channel rendering flow rates up to ≈ 680 µL min^{-1}. It was suggested that these easy to print and use devices could replace costly robotic pipettors or tedious manual pipetting procedures and lead to the design of new devices with expanded functionality. However, the operation of 3D printed pumps and valves still usually requires pneumatic actuators, so there is no improvement in the miniaturization or performance as compared to conventional electric-driven piston or peristaltic pumps and rotary valves in FI, only a change in the actuator nature. In order to foster the change of paradigm from current 'chip-in-the-lab' devices toward true 'lab-on-chip' counterparts [34], further developments should be addressed in pumping mechanisms, using e.g. electroosmotic pumps or miniaturized electric pumps [43], rather than complicating currently available fluidic drivers. Torque actuated pumps hold promise for millifluidic systems as they can be directly interfaced with a motor for unsupervised and low maintenance operation.

3. Membrane separation

The key parameters for recent applications of polymeric membranes in 3D printed devices are summarised in Table 1. It shows that commercially available membranes have successfully been incorporated into 3D printed devices for extraction and separation. For example, a commercially available Transwell® permeable support with a polycarbonate membrane was inserted above each of eight parallel flow millichannels in a simple platform

connected to a syringe pump via standard fittings to study drug transport [25]. The insert enabled molecular transport to occur from the millichannels to a reservoir above the membrane. Mammalian endothelial cells were cultured as a monolayer on the membrane surface and their viability to saponin (a cell detergent) was investigated using fluorescence microscopy on the stained membrane surface [25]. A Transwell® permeable support with a polyester membrane has also been inserted in a 3D printed millifluidic device modelled on the dimensions of a standard 96 well plate for high-throughput analysis of adenosine triphosphate released from stored erythrocytes [44]. In another application using conventional membranes, a 3D printed device incorporating an equilibrium dialysis membrane has been reported for batch studies to determine metal-protein binding constants but could potentially be incorporated in flow-through millifluidic systems. The device consisted of a printed base, containing multiple individual tailorable windows, onto which a porous dialysis membrane was manually inserted using a print-pause-print approach for seamlessly sealing the membrane onto the windows prior to being manually positioned in the base [45]. However, all of the above 3D printed devices [25, 44, 45] could be readily fabricated by micromilling and thus the potential of 3D printing is not fully demonstrated.

The possibility of 3D printing membranes in situ rather than manually inserting commercially available membranes offers great potential for on-line sample handling. One example of in situ membrane printing is based on the use of a commercially available composite filament (LayFelt®; which is part rubber–elastomeric polymer and part polyvinyl alcohol (PVA)). After printing, exposure to water removes the PVA and creates, in situ, a 3D micro-porous polymer membrane (see Fig. 1A). This procedure was applied to an integrated millifluidic system for the determination of nitrate in soil slurry containing added zinc particles (for nitrate reduction to nitrite). Nitrate from the sample chamber diffused through the membrane into a second chamber containing minute volumes of Griess reagent (15 µL) and the product was detected spectrophotometrically using a digital camera [46]. In another example, a 1 mm-thick 3D printed methacrylate functionalised PDMS membrane was incorporated in a 3D printed gas-liquid contactor using DLP in a one-step fabrication process that could not be achieved using conventional machining techniques because of the intricate configuration [47]. The efficiency of the device was demonstrated via the diffusion of CO_2 across the membrane into a bromothymol blue acid-base indicator solution.

4. Sorbent extraction/concentration

The incorporation of bead-type solid-phase extraction (SPE) media in laser lithographic or wet etched micro/milli-fluidic platforms for sample clean-up and analyte preconcentration is uncommon compared with electrokinetic methods and flow-through porous polymer monolithic phase based microextraction [48, 49]. However, the advent of 3D printing has opened up new avenues for the fabrication of automated fluidic devices with confined micro- and nano-sized bead carriers and membrane extractors, as discussed below and shown in Table 2.

In one example, a modular device integrating analyte oxidation, disk-based SPE and analyte complexation was fabricated using SLA. As proof of concept a commercial SPE disk was

manually incorporated in the device and coupled with a flow system but its applicability was only evaluated for the straightforward spectrophotometric determination of Fe(III) in water [11]. In another example, a column packed with a commercially available resin (TrisKem Pb resin) for solid phase extraction, a serpentine mixing coil (50 cm long x 1.5 mm i.d.) and a flow cell housing fibre optic cables has been applied to the spectrophotometric determination of lead in natural waters [14]. The same resin chemistry has been used for the automatic determination of metal species using a 3D printed monolithic millifluidic platform for specific assays that incorporated two columns, eight peripheral ports, and a coil with integrated baffles to enhance mixing [50], yet the fluidic platform was attached to bulk peripheral detectors.

A millifluidic FI device incorporating a 3D-printed multi-purpose injection/diverting valve stator coupled with a 3D-printed single-channel millifluidic sample preparation platform has also been reported [13]. Within the device, polyaniline decorated magnetic nanoparticles (NPs) were magnetically retained (see Fig. 1B) and used in-line for sorptive microextraction as a front end to liquid chromatography. Proof of concept was demonstrated by the determination of model emerging antimicrobial contaminants in human saliva and urine samples. There was only minimal loss of moderately non-polar compounds by adsorption on the walls of the polymeric millifluidic device, even after 20 sample injections. However, this fact unveils potential chemical incompatibility between resin and analyte/sample/reagents. To tackle this shortcoming, chemical modification of the inner surface of the channels is a promising approach.

A disposable 3D printed (using FDM), but built with user intervention, fluidic device incorporating commercial silica-based SPE has been applied to the pretreatment of non-aqueous petroleum samples (e.g. crude oil and oil-brine emulsions) for rapid breakdown of emulsions and separation of asphaltenes [51]. The printing material was PLA, and the analytical performance was similar to that achieved with silicon or glass fluidic devices, but the cost was much lower because the fabrication did not require specialized clean-room facilities for prototyping. The device remained fully functional to several solvents (e.g. n-heptane, toluene and methanol) after 20 min exposure and sample treatment times were reduced 10-fold compared with the reference centrifugation method for solvent deasphalting with quantitative recoveries of maltenes [51]. The polar filament assured good compatibility with non-polar sample matrices. This approach could in principle be extended to photoactive resins and, thus, to the other printing techniques: SLA, DLP and PIP. No study concerning ABS chemical compatibility was however presented but it is probably less tolerant to aromatic and aliphatic samples, solvents and reagents.

In all of the above examples commercially available sorbents are manually introduced into 3D printed scaffolds but a unique advantage of 3D printing is the feasibility of in situ fabrication of sorptive materials in a particle-like or mesh-like format within the interior of the device, concurrent with printing of the channel configuration. This is a consequence of the sorptive characteristics of the printing material itself for analytes, and the possibility to add nanoparticles, acting as sorbents, to liquid resins prior to printing [52]. For example, a flow-through SPE extraction device has been DLP printed containing ordered 0.4 mm cuboids made from acrylic material and used to preconcentrate metal ions by electrostatic interactions between electron donor groups on the acrylate surface and metal ions (electron acceptor groups) in solution. These cuboids were easier to print and provided

smoother surfaces than the spherical shape beads that are conventionally used in manually packed columns. The flow system gave good results for the preconcentration of Cd, Cu, Mn, Ni, Pb and Zn in seawater certified reference materials [53]. The same acrylate-based resin was also used to DLP print a knotted reactor, with square flow channels and right angled turns, which was incorporated in a conventional FI system with ICP-MS detection to determine Ag(I) ions and Ag NPs in municipal wastewater samples [40]. In this application both Ag species were "stabilised" by the addition of xanthan (a polysaccharide) and directly extracted onto the walls of the knotted reactor via hydrophobic interactions of Ag NPs and Ag(I)-complex with the reactor surface. It was shown that the retained Ag(I) ions were selectively removed at pH 12 whereas both Ag(I) ions and Ag NPs were removed at pH 10-11 but the exact chemical nature of the extraction and removal processes was not discussed. The 3D printed reactor had a 3-4-fold better extraction efficiency than a conventional knotted PTFE tube knotted reactor (each with ≈250 turns and the same volume), partly due to the greater centrifugal force exerted on the flowing stream [40]. This application exemplifies how to take advantage of the surface chemistry, but also the benefits of complex channel design that cannot be machined by traditional means.

The feasibility of fabricating novel printable SPE media has also been demonstrated by a striking application involving trapping nanosized molecularly imprinted polymer (MIP) sorbents in a 3D printed poly-ε-caprolactone (PCL) scaffold [54] that cannot be effected with conventional 10 μm-pore size polypropylene frits. The effectiveness of the device in batch mode was shown by selective SPE of alkaloid mycotoxins but the approach could also provide novel nanomaterials and nanocomposites for application in millifluidic flow systems.

From a broader perspective, the surfaces of acrylate-based channels in 3D printed fluidic scaffolds have the potential to be derivatised, e.g. with ion exchangers or chelating moieties via carbodiimide coupling of the carboxyl groups on the channel walls. This would expand their analytical utility in flow systems based on strategies reported previously for in situ chemical synthesis, capture of target species and sample preparation in flow chemistry configurations [6].

5. Chromatographic and electrophoretic separation

The advent of 3D printing has opened up the possibility of producing novel packing material not merely for on-line preconcentration but micro- and milli-fluidic separation [55]. Homogeneous particles with different geometries (e.g. truncated icosahedra (approximating spheres) and tetrahedra) have been 3D printed (using SLA) in a porous bed and the influence of morphology on plate height demonstrated [56]. The added value of this approach is that shape, orientation and packing of porous beds can be optimised using computational fluid dynamics for each application and then 3D printed.

A summary of the key characteristics of 3D printed devices incorporating chromatographic/electrophoretic separation is given in Table 3. Substrates for chromatographic applications can be 3D printed in a single step and the surface of the printed polymer substrate can be used directly (without additional functionalisation) for separations, with methacrylate and PLA based resins providing polar functionalities, and

ABS affording non-polar functionality. This approach was demonstrated (using PIP) in a planar chromatography format for the separation of visible dyes and fluorescently tagged proteins [57]. In another clever example, a millibore channel in the form of a double handed spiral (see Fig. 1C) was 3D printed using a titanium alloy cuboid [30]. The threaded connection ports were then re-tapped to ensure a good seal. The column was then subjected to a thermal polymerization in situ to be filled with a porous monolithic methacrylate based stationary phase [9] or alternatively slurry packed with reversed-phase chromatographic particles [30]. The planar structure of the printed column, together with the high thermal conductivity of titanium (compared with silica and stainless steel), enabled the column to be directly combined with a heater/cooler module for column temperature modulation [9, 30]. The monolithic-type column was used for the liquid chromatographic separation of a standard mixture of intact proteins and peptides [9]. Though the 3D printed column system only serves as a support for the stationary phase, this example demonstrates the possibility of smart printing of non-polymeric materials to exploit temperature-controlled separation in low-cost portable chromatographic systems. For further information on the role of 3D printing in separation science, including (i) a description of HPLC column geometry, (ii) characteristics of 3D printed GC columns, (iii) fabrication of thin chromatographic plates and (iv) interfaces to hyphenate separation systems with detectors, readers are referred to a recent comprehensive review by Kalsoom *et al.* [58].

Various 3D printing technologies have been used to good effect for the fabrication of millifluidic devices incorporating electrophoretic separation. For example, an affordable free-flow electrophoresis device has been fabricated using FDM with ABS resin. The device produced stable stream profiles and, as proof of principle, the separation of fluorescent dyes gave comparable separation to a glass platform [59]. An isotachophoresis system has also been 3D printed using a low cost DLP printer with an acrylate-based resin exploiting the combined benefit of the electrical insulation and optical properties of the device for the separation of three anionic dyes as a proof of principle [22].

6. Detection

Whilst 3D printed fluidic devices can be coupled to large and sophisticated detection setups (so-called "chip-in-a-lab" systems), it is an attractive proposition to integrate the detection system within the chip platform [34], particularly for remote environmental deployments and point-of-care medical use. Such an approach is well suited to millifluidic platforms incorporating optical detection based on photometry, fluorescence and chemiluminescence. For example, a photometric detector body with an integrated slit and housings for the light emitting diode source and the photodiode detector was 3D printed using FDM with black PLA resin. The integrated slit was the critical design feature to align the capillary (50 – 500 μm i.d.) transporting the sample with the optical path. Performance was benchmarked against a commercially available interface using the capillary electrophoresis separation of Zn^{2+} and Cu^{2+} complexes as a proof of concept application [60].

Fluorescence excitation and detection have also been incorporated in a 3D printed device using FDM with holders for the LED source, photodiode detector and cuvette. The source and detector were connected to the device via printed threaded ports for fibre optic cables.

The sensing device was used in batch mode, with fluidic inlet and outlet ports, and applied to the determination of metallothionein (a cancer marker) based on electromagnetic separation of immunolabelled NPs (also holder for electromagnet was 3D printed). The low-cost approach described could be used for rapid screening in place of the conventionally used enzyme-linked immunosorbent assay [61] and would appear to be easily adapted for flow through use.

The combination of sensitive chemiluminescence detection with millifluidic systems has great potential for 3D printed devices. Flow cells that could not be made using conventional milling or glass blowing can be fabricated to enhance mixing in close proximity to the detector and to match the configuration of the flow cell with the shape of the detector window to maximise light capture [12]. Radial flow cells commonly used in chemiluminescence detectors were fabricated by PIP printing and critically compared with a similarly cell designs obtained by milling. The PIP printed flow cell gave the best performance when incorporated in an FI system and computational fluid dynamic simulations indicated that this was due to a wider observation area near the flow cell inlet and lower linear velocities in the radial direction [8].

SLA and DLP printing are also viable techniques for producing microfluidic components for flow through electrochemical detection. For example, a flow cell was assembled simply by placing a 3D fabricated component (containing the reference electrode) on top of a base plate, which acted as the working electrode, and binding the two components together with cotton thread. This configuration allowed a wide range of working electrode materials to be tested and offers a high degree of design flexibility, and high reliability compared with conventional fabrication techniques [62]. Cardoso *et al.* [63] have recently demonstrated the potential of FDM for low-cost fabrication of 3D printed electrodes using conductive graphene-doped filaments that are amenable to 3D fabricated multi-purpose electrochemical cells for voltammetric and amperometric FI and batch injection analysis.

Also, inexpensive cyclonic spray chambers for ICP applications [64, 65] have been PLA (FDM) and acrylate-resin (SLA) printed for substituting the commercial quartz counterparts. This application showcases the flexibility and wide application of 3D printing in the analytical chemistry context due to its capabilities of producing bespoke components for most unexpected tasks using currently available printable materials.

7. Future Perspectives

3D printing will continue to open up new opportunities for analytical instrumentation, including the design of components and the application of millifluidic flow through devices, without the need for specialized facilities such as clean-room environments. The ability to design, print, and modify the device within hours is a very powerful capability. When computational fluid dynamics is used to simulate flow regimes within the device the design can be rapidly optimised, and all of this can be done "in house" at relatively low cost.

The advent of 3D printed multiplex fluidic platforms able to include several external components, such as electronic chips, membranes or active materials (e.g., conductive inks)

to name a few, will further expand this cutting-edge technology and foster the miniaturization, portability and connectivity of the designed devices, with on-chip integration of the detection step via optical or electrochemical methods for in-field and point-of-care analysis.

With regard to specific design features, various millifluidic flow components for unit operations (e.g. valves, pumps, mixers, reactors, sorptive and chromatographic phases, membranes, and detector housings) can be fabricated, either separately or combined in one-step 3D printed platforms. Further developments in this context can be expected as desktop printers become available with higher resolution at affordable prices.

Most of the publications to date have demonstrated proof-of-concept studies for a variety of ingenious fluidic platform/scaffold designs and have used simple applications for that purpose. The next step is to expand the applicability and scope of 3D printed milli/microfluidic platforms to more challenging sample matrices and analytical problems. One strategy to accomplish this is to import technologies from related areas. As one example, liquid-phase extraction/microextraction has not yet been reported in this arena despite the fact that the feasibility of combining organic solvents with FDM and SLM printed fluidic structures for short contact times has been established.

The availability and use of custom-formulations (e.g. blends and materials/curable resins) is also expected in the not too distant future and this will improve the range of physical and chemical characteristics that can be incorporated in 3D printed devices, e.g. through the use of sintered glass, metals and nanocomposites. These new formulations will also help to address issues associated with leaching and/or adsorption of target analytes to the printed structures. It may also facilitate faster post-print curing of photopolymerised devices. These materials will be welcome even if further postprinting processing is required (e.g. casting, sintering), because in many instances, the most striking benefits of 3D printing are its enabling capabilities for designing complex structures. Likewise, new approaches for tailoring the surface chemistry can be expected for dedicated applications.

Regarding the transferability of research prototypes, the rapid fabrication of low cost fit-for-purpose millifluidic analytical systems, deployment in developing countries and use in remote locations has received limited coverage to date but undoubtedly there is considerable scope for further development in each of these areas. 3D printing in the industrial domain is not yet a competitive alternative to subtractive technology due to the running costs of current proprietary resins compared with milling substrates, limited availability of materials and low throughput; increasing the performance of printers will allow their entry into that domain.

Figure captions

Figure 1. A conceptual FI manifold showing examples of 3D printed devices for on-line membrane separation (A), sorbent extraction/concentration (B) and chromatographic separation (C). Fig. 1A is reprinted with permission from [46], Copyright 2017, American Chemical Society. Fig. 1C is reprinted from [9] with permission from Elsevier.

Figure 2. 3D printed millifluidic mixers and reactors for FI applications. From left to right; a serpentine T-piece mixer (volume ca. 60 µL), a cuboid mixer (volume 1000 µL) and a lab-on-valve stator for multiplex assays. A one euro coin is also shown for size comparison.

References

[1]   Y. He, Y. Wu, J.Z. Fu, Q. Gao, J.J. Qiu, Developments of 3D Printing Microfluidics and Applications in Chemistry and Biology: a Review, Electroanalysis, 28 (2016) 1658-1678.

[2]   A.K. Au, W. Huynh, L.F. Horowitz, A. Folch, 3D-Printed Microfluidics, Angewandte Chemie - International Edition, 55 (2016) 3862-3881.

[3]   G.W. Bishop, J.E. Satterwhite-Warden, K. Kadimisetty, J.F. Rusling, 3D-printed bioanalytical devices, Nanotechnology, 27 (2016).

[4]   B. Gross, S.Y. Lockwood, D.M. Spence, Recent advances in analytical chemistry by 3D printing, Analytical Chemistry, 89 (2017) 57-70.

[5]   G.I.J. Salentijn, P.E. Oomen, M. Grajewski, E. Verpoorte, Fused Deposition Modeling 3D Printing for (Bio)analytical Device Fabrication: Procedures, Materials, and Applications, Analytical Chemistry, 89 (2017) 7053-7061.

[6]   M.D. Symes, P.J. Kitson, J. Yan, C.J. Richmond, G.J.T. Cooper, R.W. Bowman, T. Vilbrandt, L. Cronin, Integrated 3D-printed reactionware for chemical synthesis and analysis, Nature Chemistry, 4 (2012) 349-354.

[7]   S. Waheed, J.M. Cabot, N.P. Macdonald, T. Lewis, R.M. Guijt, B. Paull, M.C. Breadmore, 3D printed microfluidic devices: Enablers and barriers, Lab on a Chip, 16 (2016) 1993-2013.

[8]   V. Gupta, P. Mahbub, P.N. Nesterenko, B. Paull, A new 3D printed radial flow-cell for chemiluminescence detection: Application in ion chromatographic determination of hydrogen peroxide in urine and coffee extracts, Analytica Chimica Acta, (2018).

[9]   V. Gupta, M. Talebi, J. Deverell, S. Sandron, P.N. Nesterenko, B. Heery, F. Thompson, S. Beirne, G.G. Wallace, B. Paull, 3D printed titanium micro-bore columns containing polymer monoliths for reversed-phase liquid chromatography, Analytica Chimica Acta, 910 (2016) 84-94.

[10]   S. Mardani, L.S. Ojala, P. Uusi-Kyyny, V. Alopaeus, Development of a unique modular distillation column using 3D printing, Chemical Engineering and Processing: Process Intensification, 109 (2016) 136-148.

[11]   C. Calderilla, F. Maya, V. Cerdà, L.O. Leal, 3D printed device including disk-based solid-phase extraction for the automated speciation of iron using the multisyringe flow injection analysis technique, Talanta, 175 (2017) 463-469.

[12]   K.B. Spilstead, J.J. Learey, E.H. Doeven, G.J. Barbante, S. Mohr, N.W. Barnett, J.M. Terry, R.M. Hall, P.S. Francis, 3D-printed and CNC milled flow-cells for chemiluminescence detection, Talanta, 126 (2014) 110-115.

[13]   H. Wang, D.J. Cocovi-Solberg, B. Hu, M. Miró, 3D-Printed Microflow Injection Analysis Platform for Online Magnetic Nanoparticle Sorptive Extraction of Antimicrobials in Biological Specimens as a Front End to Liquid Chromatographic Assays, Analytical Chemistry, 89 (2017) 12541-12549.

[14]   E. Mattio, F. Robert-Peillard, C. Branger, K. Puzio, A. Margaillan, C. Brach-Papa, J. Knoery, J.L. Boudenne, B. Coulomb, 3D-printed flow system for determination of lead in natural waters, Talanta, 168 (2017) 298-302.

[15]   L.A. Porter, Jr., C.A. Chapman, J.A. Alaniz, Simple and inexpensive 3D printed filter fluorometer designs: User-friendly instrument models for laboratory learning and outreach activities, Journal of Chemical Education, 94 (2017) 105-111.

[16]   V. Cerdà, J. Avivar, D. Moreno, Chips: How to build and implement fluidic devices in flow based systems, Talanta, 166 (2017) 412-419.

[17]   C.M.B. Ho, S.H. Ng, K.H.H. Li, Y.J. Yoon, 3D printed microfluidics for biological applications, Lab on a Chip, 15 (2015) 3627-3637.

[18]   Y. Zhang, S. Ge, J. Yu, Chemical and biochemical analysis on lab-on-a-chip devices fabricated using three-dimensional printing, Trends in Analytical Chemistry, 85 (2016) 166-180.

[19]   C.L. Manzanares Palenzuela, M. Pumera, (Bio)Analytical chemistry enabled by 3D printing: Sensors and biosensors, Trends in Analytical Chemistry, 103 (2018) 110-118.

[20]   S.G. Jeong, S.H. Lee, C.H. Choi, J. Kim, C.S. Lee, Toward instrument-free digital measurements: A three-dimensional microfluidic device fabricated in a single sheet of paper by double-sided printing and lamination, Lab on a Chip, 15 (2015) 1188-1194.

[21]   P. Juskova, A. Ollitrault, M. Serra, J.-L. Viovy, L. Malaquin, Resolution improvement of 3D stereo-lithography through the direct laser trajectory programming: Application to microfluidic deterministic lateral displacement device, Analytica Chimica Acta, 1000 (2018) 239-247.

[22]   A.I. Shallan, P. Smejkal, M. Corban, R.M. Guijt, M.C. Breadmore, Cost-effective three-dimensional printing of visibly transparent microchips within minutes, Analytical Chemistry, 86 (2014) 3124-3130.

[23]   M. Villegas, Z. Cetinic, A. Shakeri, T.F. Didar, Fabricating smooth PDMS microfluidic channels from low-resolution 3D printed molds using an omniphobic lubricant-infused coating, Analytica Chimica Acta, 1000 (2018) 248-255.

[24] M.J. Beauchamp, G.P. Nordin, A.T. Woolley, Moving from millifluidic to truly microfluidic sub-100-μm cross-section 3D printed devices, Analytical and Bioanalytical Chemistry, 409 (2017) 4311-4319.

[25] K.B. Anderson, S.Y. Lockwood, R.S. Martin, D.M. Spence, A 3D printed fluidic device that enables integrated features, Analytical Chemistry, 85 (2013) 5622-5626.

[26] R. Amin, S. Knowlton, A. Hart, B. Yenilmez, F. Ghaderinezhad, S. Katebifar, M. Messina, A. Khademhosseini, S. Tasoglu, 3D-printed microfluidic devices, Biofabrication, 8 (2016).

[27] A.M. Tothill, M. Partridge, S.W. James, R.P. Tatam, Fabrication and optimisation of a fused filament 3D-printed microfluidic platform, Journal of Micromechanics and Microengineering, 27 (2017).

[28] N.P. Macdonald, J.M. Cabot, P. Smejkal, R.M. Guijt, B. Paull, M.C. Breadmore, Comparing Microfluidic Performance of Three-Dimensional (3D) Printing Platforms, Analytical Chemistry, 89 (2017) 3858-3866.

[29] H. Gong, B.P. Bickham, A.T. Woolley, G.P. Nordin, Custom 3D printer and resin for 18 μm × 20 μm microfluidic flow channels, Lab on a Chip, 17 (2017) 2899-2909.

[30] S. Sandron, B. Heery, V. Gupta, D.A. Collins, E.P. Nesterenko, P.N. Nesterenko, M. Talebi, S. Beirne, F. Thompson, G.G. Wallace, F. Regan, B. Paull, 3D printed metal columns for capillary liquid chromatography, Analyst, 139 (2014) 6343-6347.

[31] C.K. Su, S.C. Yen, T.W. Li, Y.C. Sun, Enzyme-Immobilized 3D-Printed Reactors for Online Monitoring of Rat Brain Extracellular Glucose and Lactate, Analytical Chemistry, 88 (2016) 6265-6273.

[32] N. Ollivier, E. Mattio, B. Coulomb, D. Bonne, F. Robert-Peillard, J.L. Boudenne, Modified 3D-printed device for mercury determination in waters, 21st International Conference on Flow Injection Analysis and Related Techniques, Book of AbstractsSt Petersburg, Russia, 2017, pp. 113.

[33] N. Bhattacharjee, A. Urrios, S. Kang, A. Folch, The upcoming 3D-printing revolution in microfluidics, Lab on a Chip, 16 (2016) 1720-1742.

[34] H.N. Chan, Y. Shu, B. Xiong, Y. Chen, Y. Chen, Q. Tian, S.A. Michael, B. Shen, H. Wu, Simple, Cost-Effective 3D Printed Microfluidic Components for Disposable, Point-of-Care Colorimetric Analysis, ACS Sensors, 1 (2016) 227-234.

[35] C.K. Su, S.C. Hsia, Y.C. Sun, Three-dimensional printed sample load/inject valves enabling online monitoring of extracellular calcium and zinc ions in living rat brains, Analytica Chimica Acta, 838 (2014) 58-63.

[36] H. Gong, A.T. Woolley, G.P. Nordin, High density 3D printed microfluidic valves, pumps, and multiplexers, Lab on a Chip, 16 (2016) 2450-2458.

[37] S.J. Keating, M.I. Gariboldi, W.G. Patrick, S. Sharma, D.S. Kong, N. Oxman, 3D printed multimaterial microfluidic valve, PLoS ONE, 11 (2016).

[38] C.I. Rogers, K. Qaderi, A.T. Woolley, G.P. Nordin, 3D printed microfluidic devices with integrated valves, Biomicrofluidics, 9 (2015).

[39] A.K. Au, N. Bhattacharjee, L.F. Horowitz, T.C. Chang, A. Folch, 3D-printed microfluidic automation, Lab on a Chip, 15 (2015) 1934-1941.

[40] C.K. Su, M.H. Hsieh, Y.C. Sun, Three-dimensional printed knotted reactors enabling highly sensitive differentiation of silver nanoparticles and ions in aqueous environmental samples, Analytica Chimica Acta, 914 (2016) 110-116.

[41] P.J. Kitson, M.H. Rosnes, V. Sans, V. Dragone, L. Cronin, Configurable 3D-Printed millifluidic and microfluidic 'lab on a chip' reactionware devices, Lab on a Chip, 12 (2012) 3267-3271.

[42] V. Dragone, V. Sans, M.H. Rosnes, P.J. Kitson, L. Cronin, 3D-printed devices for continuous-flow organic chemistry, Beilstein Journal of Organic Chemistry, 9 (2013) 951-959.

[43] D.A. Henderson, Novel Piezo Motor Enables Positive Displacement Microfluidic Pump, 2007, pp. 272-275.

[44] C. Chen, Y. Wang, S.Y. Lockwood, D.M. Spence, 3D-printed fluidic devices enable quantitative evaluation of blood components in modified storage solutions for use in transfusion medicine, Analyst, 139 (2014) 3219-3226.

[45] C.W. Pinger, A.A. Heller, D.M. Spence, A Printed Equilibrium Dialysis Device with Integrated Membranes for Improved Binding Affinity Measurements, Analytical Chemistry, 89 (2017) 7302-7306.

[46] F. Li, P. Smejkal, N.P. Macdonald, R.M. Guijt, M.C. Breadmore, One-Step Fabrication of a Microfluidic Device with an Integrated Membrane and Embedded Reagents by Multimaterial 3D Printing, Analytical Chemistry, 89 (2017) 4701-4707.

[47] T. Femmer, A.J.C. Kuehne, M. Wessling, Print your own membrane: Direct rapid prototyping of polydimethylsiloxane, Lab on a Chip, 14 (2014) 2610-2613.

[48] M. Sonker, V. Sahore, A.T. Woolley, Recent advances in microfluidic sample preparation and separation techniques for molecular biomarker analysis: A critical review, Analytica Chimica Acta, 986 (2017) 1-11.

[49]   B.C. Giordano, D.S. Burgi, S.J. Hart, A. Terray, On-line sample pre-concentration in microfluidic devices: A review, Analytica Chimica Acta, 718 (2012) 11-24.

[50]   E. Mattio, F. Robert-Peillard, L. Vassalo, C. Branger, A. Margaillan, C. Brach-Papa, J. Knoery, J.L. Boudenne, B. Coulomb, 3D-printed lab-on-valve for fluorescent determination of cadmium and lead in water, Talanta, 183 (2018) 201-208.

[51]   E.M. Kataoka, R.C. Murer, J.M. Santos, R.M. Carvalho, M.N. Eberlin, F. Augusto, R.J. Poppi, A.L. Gobbi, L.W. Hantao, Simple, Expendable, 3D-Printed Microfluidic Systems for Sample Preparation of Petroleum, Analytical Chemistry, 89 (2017) 3460-3467.

[52]   C.K. Su, W.C. Chen, 3D-printed, TiO2 NP–incorporated minicolumn coupled with ICP-MS for speciation of inorganic arsenic and selenium in high-salt-content samples, Microchimica Acta, 185 (2018).

[53]   C.K. Su, P.J. Peng, Y.C. Sun, Fully 3D-Printed Preconcentrator for Selective Extraction of Trace Elements in Seawater, Analytical Chemistry, 87 (2015) 6945-6950.

[54]   G. De Middeleer, P. Dubruel, S. De Saeger, Molecularly imprinted polymers immobilized on 3D printed scaffolds as novel solid phase extraction sorbent for metergoline, Analytica Chimica Acta, 986 (2017) 57-70.

[55]   C. Fee, S. Nawada, S. Dimartino, 3D printed porous media columns with fine control of column packing morphology, Journal of Chromatography A, 1333 (2014) 18-24.

[56]   S. Nawada, S. Dimartino, C. Fee, Dispersion behavior of 3D-printed columns with homogeneous microstructures comprising differing element shapes, Chemical Engineering Science, 164 (2017) 90-98.

[57]   N.P. Macdonald, S.A. Currivan, L. Tedone, B. Paull, Direct Production of Microstructured Surfaces for Planar Chromatography Using 3D Printing, Analytical Chemistry, 89 (2017) 2457-2463.

[58]   U. Kalsoom, P.N. Nesterenko, B. Paull, Current and future impact of 3D printing on the separation sciences, Trends in Analytical Chemistry, 105 (2018) 492-502.

[59]   S.K. Anciaux, M. Geiger, M.T. Bowser, 3D Printed Micro Free-Flow Electrophoresis Device, Analytical Chemistry, 88 (2016) 7675-7682.

[60]   F. Cecil, M. Zhang, R.M. Guijt, A. Henderson, P.N. Nesterenko, B. Paull, M.C. Breadmore, M. Macka, 3D printed LED based on-capillary detector housing with integrated slit, Analytica Chimica Acta, 965 (2017) 131-136.

[61] Z. Heger, J. Zitka, N. Cernei, S. Krizkova, M. Sztalmachova, P. Kopel, M. Masarik, P. Hodek, O. Zitka, V. Adam, R. Kizek, 3D-printed biosensor with poly(dimethylsiloxane) reservoir for magnetic separation and quantum dots-based immunolabeling of metallothionein, Electrophoresis, 36 (2015) 1256-1264.

[62] M.E. Snowden, P.H. King, J.A. Covington, J.V. MacPherson, P.R. Unwin, Fabrication of versatile channel flow cells for quantitative electroanalysis using prototyping, Analytical Chemistry, 82 (2010) 3124-3131.

[63] R.M. Cardoso, D.M.H. Mendonça, W.P. Silva, M.N.T. Silva, E. Nossol, R.A.B. da Silva, E.M. Richter, R.A.A. Muñoz, 3D printing for electroanalysis: From multiuse electrochemical cells to sensors, Analytica Chimica Acta, (2018), in the press. DOI: 10.1016/j.aca.2018.06.021

[64] V. Geertsen, E. Barruet, O. Taché, 3D printing for cyclonic spray chambers in ICP spectrometry, Journal of Analytical Atomic Spectrometry, 30 (2015) 1369-1376.

[65] D.F. Thompson, Rapid production of cyclonic spray chambers for inductively coupled plasma applications using low cost 3D printer technology, Journal of Analytical Atomic Spectrometry, 29 (2014) 2262-2266.

[66] M.M. Wang, P. Laborda, L.P. Conway, X.C. Duan, K. Huang, L. Liu, J. Voglmeir, An integrated 3D-printed platform for the automated isolation of N-glycans, Carbohydrate Research, 433 (2016) 14-17.

eparation

Commercial or fabricated membrane	Membrane material	Printer / print technology	Print material	Component dimensions	Application	Comments	Reference
Commercial	Transwell® polycarbonate (0.4 µm pore size)	Objet Connex 350, Stratasys Ltd / PIP	Objet Vero White Plus® (acrylate based)	Membrane diameter 6.5 mm; flow channels 3 mm wide × 1.5 mm deep	Drug transport	Detection by fluorescence microscopy, HPLC-ESI-MS/MS	[25]
Commercial	Transwell® polyester (0.4 µm pore size)	Objet Connex 350, Stratasys Ltd / PIP	Objet VeroClear® (acrylate based)	Membrane 6.5 mm diameter; flow channels 2.0 mm wide × 2.0 mm deep	ATP release from erythrocytes	Modelled on a 96 well plate, luciferin-luciferase chemiluminescence assay	[44]
Commercial	Regenerated-cellulose dialysis membrane, molecular-weight cut-off ≈3500 Da	Objet Connex 350, Stratasys Ltd / PIP	VeroClear® (acrylate based)	Membrane holders 3.3 mm wide × 32.8 mm long inserted into a printed base resembling a well plate configuration	Metal-protein binding constants	Modelled on a 96 well plate, detection by liquid scintillation	[45]
Fabricated	LayFelt® and polyvinyl alcohol	Dual extruder FELIX 3D, Felix	ABS, PLA and lay-felt	Membrane 29 mm long × 1.6 mm thick × 0.4	Nitrate in soil slurry using	Spectrophotometric detection using a	[46]

	(0.2 – 0.7 mm thick)	Printers / FDM		mm wide; channels 20 mm long × 0.7 mm deep × 1 mm wide	Griess reagents	digital camera	
Fabricated	PDMS (1 mm thick)	Perfactory Minimultilense, EnvisionTEC / DLP	Custom PDMS photoresist (97.95% (methacryloxypropyl methylsiloxane)-dimethylsiloxane copolymer, 2% ethyl(2,4,6-trimethylbenzoyl)phenyl phosphinate as a photoinitiator incorporating 0.05 wt% Orasol Orange dye)	Channel width 150 – 400 µm	Diffusion of CO_2 into acid/base indicator	Rapid prototyping of gas permeable device	[47]
Commercial	Semipermeable dialysis membrane	MakerBot Replicator 2/FDM	PLA	Tubing adapted to 96-well plate configuration	Isolation of N-glycans from glycoproteins	Modular 3D printed platform with integrated dispersive solid-phase extraction for trapping of liberated oligosaccharides	[66]

2), Digital Light Processing; ABS, Acrylonitrile-butadiene-
3 erformance Liquid Chromatography-Electrospray
4
5

ction/concentration

Commercial or fabricated extraction phase	SPE material	Printer / print technology	Print material	Component dimensions	Application	Comments	Reference
Commercial	Chelating membrane disks (Empore, 3M)	Form 1+, Formlabs Inc /SLA	Clear Photoactive®	Membrane support 7 mm diameter	Speciation of Fe in groundwater	Only coupled to spectrophotometric detection, not to atomic spectrometry	[11]
Commercial	TriSKem Pb resin	Form 1+, Formlabs Inc/SLA	Acrylic resin	Column dimensions not stated	Lead in natural waters	Spectrophotometric detection with 4-(2-pyridylazo)-resorcinol	[14]
Commercial	TriSKem Pb resin and Amberlite® IR 120 (for Cd)	Form 1+, Formlabs Inc/SLA	Acrylic epoxy resins (Veroclear®; / FLGPCL02; BV-007)	50 mg resin in each column. Dimensions not stated	Cadmium and lead in water	Three 3D printing techniques compared (SLA, PIP and DLP)	[50]
		Object500 Connex 3, Stratasys Ltd /PIP	SUP706 soluble support				
		Miicraft 100, Rays Optics Inc. / DLP					

Fabricated	Polyaniline decorated magnetic nanoparticles	Form 2, Formlabs Inc/ SLA	LGPCL02	SPE chamber 50 mm long × 3 mm wide × 0.8 mm high	Antimicrobials (alkyl esters of 4-hydroxybenzoic acid and triclosan) in biological specimens	Fully automatic sample preparation using a functional 3D printed valve and on-line hyphenation to HPLC	[13]
Commercial	200 mg of Celite® 545 (diatomaceous earth)	Graber i3, GTMax3D / FDM	PLA	SPE chamber ≈ 14 mm long × 6 mm wide × 7 mm high; chip dimensions 50 mm long × 25 mm wide × 10 mm high.	Pretreatment of petroleum samples (emulsion breaking and removal of asphaltenes in heptane)	3D printed chamber dry packed with SPE phase. PLA, PTFE and Celite compared for analyte sorption	[51]
Fabricated in situ (3D printed)	0.4 mm acrylic cuboids	MiiCraft® / DLP	BV-001 (acrylate based)	526 cuboids (29 layers) each of 0.4 mm × 0.2 mm × 0.4 mm (width × height × length)	Trace elements in seawater (salt removal)	FI with ICP-MS detection	[53]
Fabricated in situ (3D printed)	acrylic "knotted reactor"	MiiCraft® / DLP	BV-001 (acrylate based)	Each turn 1 mm × 1 mm × 3 mm (width × height × length); 128-768 right angle turns	Ag NPs and Ag(I) ions in wastewater	FI with ICP-MS detection	[40]

Fabricated in situ (3D printed)	Nanosized MIP immobilized onto 3D printed structures	Bioplotter™, EnvisionTEC / syringe based extrusion	PCL	10 mm high × 9 mm diameter PCL scaffold	Metergoline as a model template for ergot alkaloid mycotoxins	Empty 3 mL Bond Elut SPE cartridge filled with MIP functionalised PCL scaffold (height 10 mm, diameter 9 mm)	[54]
Fabricated (3D printed) and packed in printed column holders	TiO$_2$-nanoparticle incorporated cuboid-stacked phase	MiiCraft 125/DLP	BV-007 resin incorporating 1% TiO$_2$ nanoparticles	150 cuboids (30 layers) each of 0.3 mm × 0.3 mm × 2.7 mm (width × height × length)	Non-chromatographic speciation of As(III)/As(V) and Se(IV)/Se(VI) by pH adjustment	FI with ICP-MS detection	[52]

7 , Digital Light Processing; SLA: Stereolithography; PCL:
8 d Plasma-Mass spectrometry

9

10

...phic / electrophoretic separation

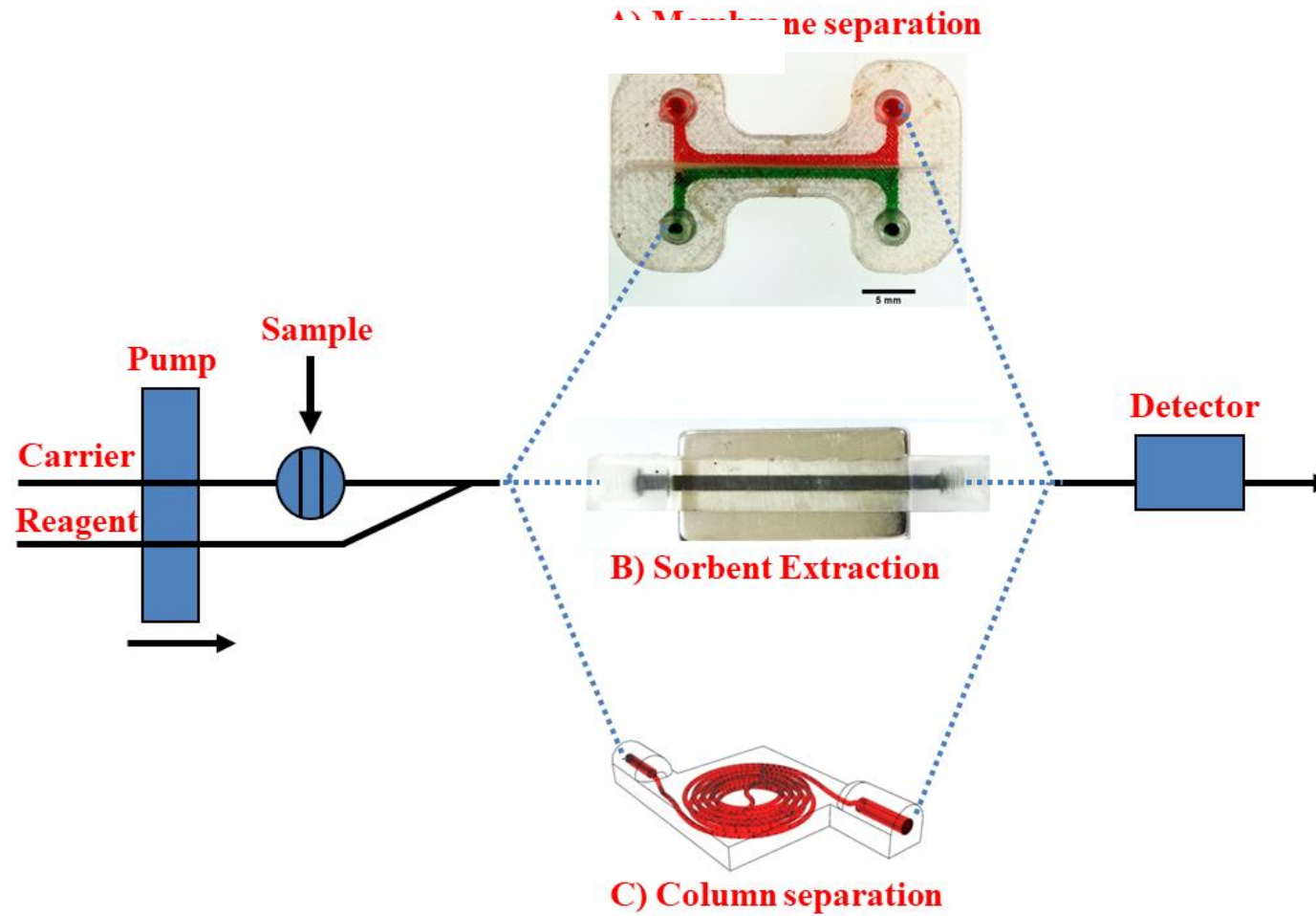| Configuration	Printer / print technology	Print material	Dimensions	Application	Comments	Reference
Planar separation plate	Objet Eden 260VS, Stratasys Ltd / PIP	VeroClear® RGD810	53 mm long × 17.3 µm deep × 11.9 µm wide	Fluorescent dyes and fluorescently tagged proteins	Unfunctionalised polymer thin layer chromatography platforms	[57]
Double spiral shaped column	Realizer SLM-50™ / SLM	Powdered metal (titanium alloy, Ti-6Al-4V) platform. Poly(butyl methacrylate-co-ethyleneglycol-dimethacrylate) monolithic stationary phase	60 cm long × 0.9 mm i.d.	Intact proteins and peptides from complex mixtures	Stationary phase thermally polymerised. Used with real time temperature modulation	[9]
Planar separation channel	Ultimaker / FDM	ABS	2.5 cm long × 80 µm deep × 1 cm wide	Fluorescent dyes; myoglobin and cytochrome c	Free-flow electrophoresis	[59]
Serpentine separation channel	Miicraft® / DLP	Proprietary acrylate/epoxy resin	10 cm long × 1.0 mm deep × 500 µm wide	Three anionic dyes	Isotachophoresis	[22]

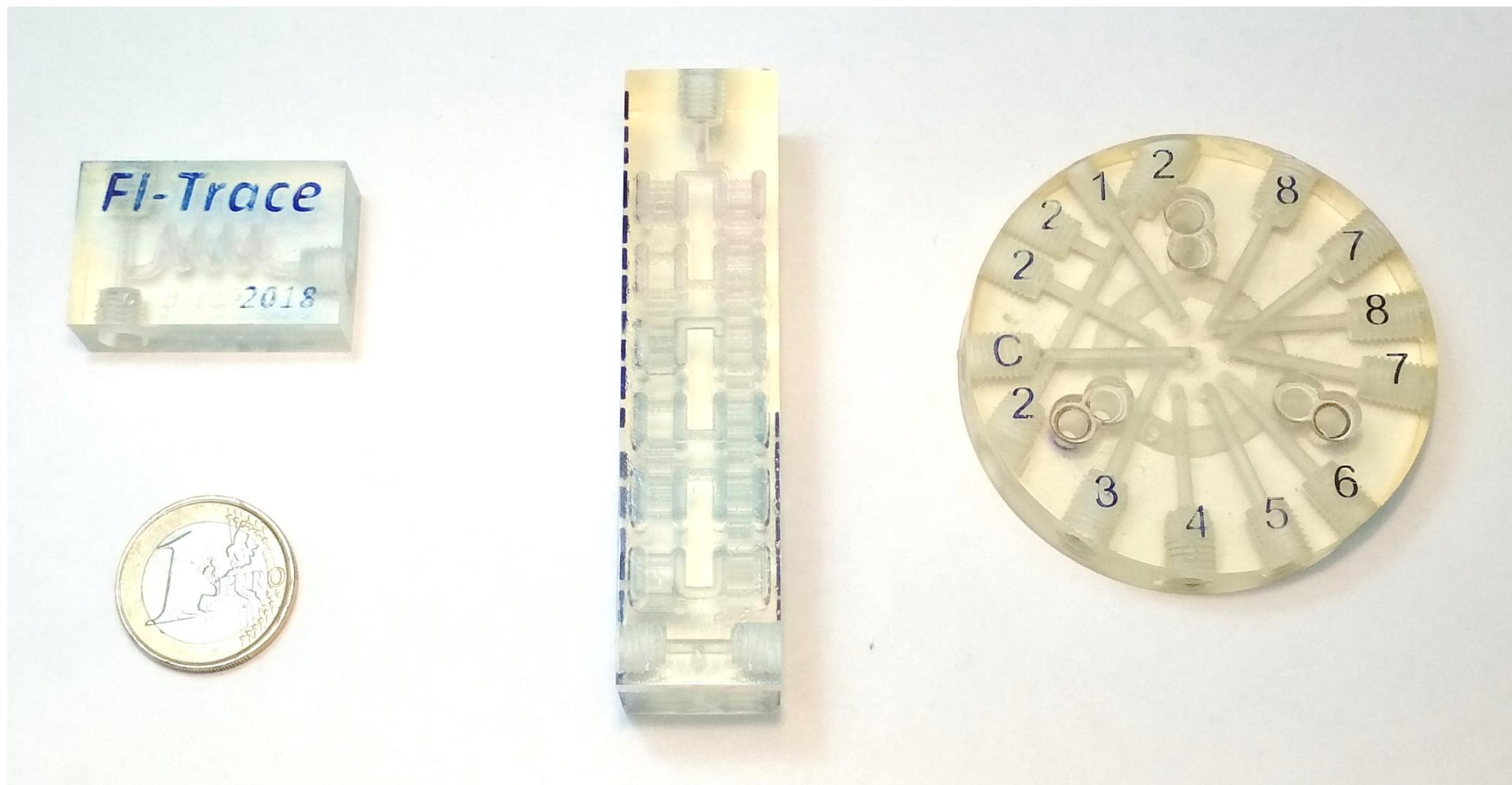DLP, Digital Light Processing; ABS, Acrylonitrile-butadiene-

14

15

16

A) Membrane separation

B) Sorbent Extraction

C) Column separation

Pump

Sample

Carrier

Reagent

Detector

18

19